

# Friction Velocity from Active Thermography and Shape Analysis

Christoph S. Garbe and Alexander Heinlein

*Interdisciplinary Center for Scientific Computing (IWR), University of Heidelberg,  
Speyerer Str. 6, 69115 Heidelberg, Germany E-mail: christoph.garbe@iwr.uni-heidelberg.de*

**Abstract.** A novel technique is presented that makes it feasible to measure the viscous shear stress  $\tau_\mu$  from active thermography. With a CO<sub>2</sub> laser, patterns are written to the sea surface. This temperature structure is distorted by the velocity profile in the viscous boundary layer. Due to the non-zero penetration depth of both the laser and the infrared camera, this vertical velocity profile can be resolved. The viscous shear stress is extracted from the recovered velocity profile. The computation relies on a shape analysis of the visualized thermal structures. An analytical function is derived which captures the dynamical processes. The model parameters can then be computed in a standard nonlinear parameter estimation framework. This novel technique is tested both on simulated data and on measurements conducted in a small annular wind-wave flume. The friction velocity computed in this fashion compared favorably to independent measurements. Although not tested yet, this technique should be equally applicable to field measurements.

Key Words: viscous shear stress, active thermography

## 1. Introduction

The transport of energy, momentum and mass across the air-sea interface are central questions in the study of air-sea interaction and ocean atmosphere modeling. A long standing effort has been put into measuring the transfer of mass across the air water interface (Liss and Slater 1974; Broecker and Peng 1974, 1982, Jähne *et al.* 1987; Watson *et al.* 1991) as well as parameterizing this transfer (Liss and Merlivat 1986; Wanninkhof 1992; Wanninkhof *et al.* 1993; Wanninkhof and McGillis 1999). Due to the advantages of using heat as a proxy for mass transfer, research has been undertaken to scale from the transfer velocity of heat to that of gas (Jähne *et al.* 1989; Haußecker *et al.* 1995, 2001; Schimpf *et al.* 2004; Atmane *et al.* 2004). A review on the subject of air-water mass transfer can be found in Jähne and Haußecker (1998) and more recently in Wanninkhof *et al.* (2009).

Apart from the transport of energy and mass, the transport of momentum is of

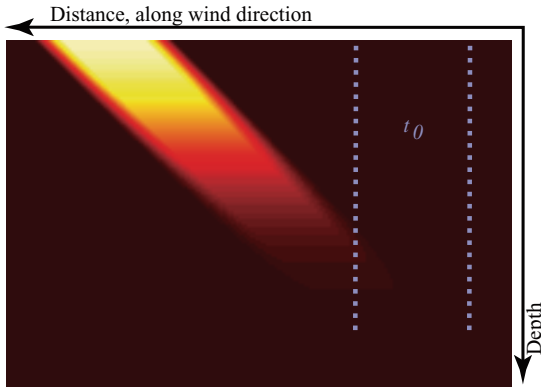


**Figure 1** Sheared heat structure at a given time after having been written, viewed from the side (Garbe *et al.* 2007)

great importance for ocean-atmosphere modeling as well as for understanding the processes at the air-sea interface. The transport of momentum from atmosphere to ocean is the driving force in a number of interfacial processes. Generally, the momentum flux  $\tau$  is partitioned into viscous stress  $\tau_\mu$  and wave induced stress  $\tau_w$ . The wave induced stress, also known as form stress, is due to the pressure force acting on the slope of waves. This stress  $\tau_w$  is strongly connected to the wave age  $\beta$ , which is defined as the momentum transfer rate from wind to waves per unit wave momentum. An analysis of this quantity in the air-sea momentum flux budget analysis can be found in Kukulka and Hara (2005). Recently, Mueller and Veron (2009) demonstrated the effect of flow separation on the surface stress due to the wave field. This makes spatially highly resolved measurements of this quantity important. Measurements of the heat transfer and the viscous shear flux in the same footprint spatially resolved are important for gaining insights into transport mechanisms.

Banner and Peirson (1998) conducted experiments and tried to measure the partition of the total momentum transfer into the viscous and the wave-induced stress. Contrary to Okuda *et al.* (1977) they found a large partition of more than 50% of the total momentum transfer to be made up by the wave-induced stress. More recently Uz *et al.* (2002) found the partition of total momentum flux to wave induced stress to be 64% for typical conditions. This figure is in close agreement to the results published by Banner and Peirson (1998).

While Okuda *et al.* (1977) measured the viscous stress  $\tau_\mu$  from hydrogen bubbles, Banner and Peirson (1998) performed their tangential stress measurements with a PIV technique using particles of diameters ranging from 20-60  $\mu\text{m}$ . The discrepancy in the results between Okuda *et al.* (1977) and Banner and Peirson (1998) can be attributed to a large part in uncertainties in the use of

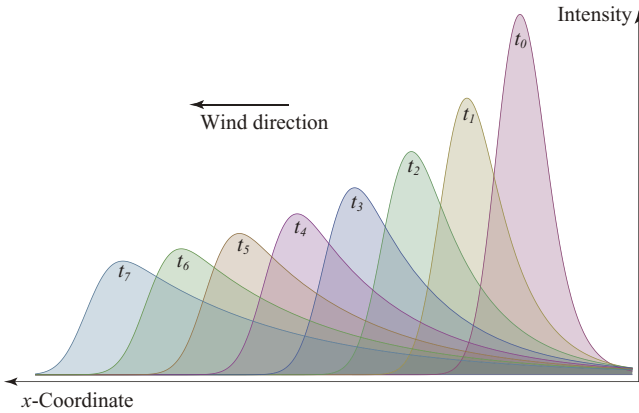


**Figure 2** The time progression of the analytical function from Eqn. (2).

hydrogen bubbles for the flow visualization. The resulting bubbles in measurements by Okuda *et al.* (1977) and McLeish and Putland (1975) before them are quite large leading to a number of difficulties, as detailed by Banner and Peirson (1998).

Previous measurements of the viscous shear relied on particle based PIV measurements. This type of approach is not applicable to field conditions. This represents a significant drawback and opens room for further investigations. In this contribution, a novel technique will be presented that relies on active thermography for measuring the viscous stress from single images. Underlying to this technique is the assumption that the Blasius velocity profile at the air-water interface can be approximated by a linear velocity profile to the depth relevant for IR radiation. Information concerning the velocity structure with depth cannot be recovered from passive thermography. Therefore, active thermography is necessary, as shall be described in the next section.

## 2. Modeling the viscous boundary layer

The estimation of the velocity gradient in the viscous boundary layer from active thermography is a classical inverse problem. As such, model assumptions have to be made and the model parameters have to be computed from the image data.

Let the  $xy$ -plane be parallel to the water surface at  $z=0$ , the wind is blowing in positive  $x$ -direction. The underlying model assumption of our presented technique is that of the Blasius velocity profile at the air-water interface, which can be accurately approximated by a linear velocity profile  $u(z)$  with depth  $z$  within the penetration depth or IR radiation. This velocity profile  $u(z)$  leads to a shearing of

thermal structures written into the viscous boundary layer. Our model assumptions are as follows:

1. The Blasius velocity profile at the air-water interface can be approximated by a linear velocity profile  $u(z) = u_0 \cdot G \cdot z$  up to a depth relevant for IR radiation. Here  $u_0 = u(z=0)$  is the velocity directly at the surface and  $G = \partial u / \partial z$  is the velocity gradient.
2. A CO<sub>2</sub> laser with a Gaussian beam profile is used for heating up a three dimensional water volume. The depth of this heated up water volume is defined by the penetration depth of the radiation into water.
3. The heat applied to the surface at  $z=0$  results in a visualized temperature  $T(x, y) = T_0 \cdot e^{-(x-x')^2/2\sigma^2}$  with the width of the Gaussian bell curve  $\sigma$  and the location of the peak temperature at  $x'$ .
4. Due to the strong absorption of infrared radiation in water, the absorption with depth  $z$  is described by Lambert-Beer's law. The heat deposited with depth leads to a temperature profile with the functional form  $T(z) = T_0 e^{-\beta z}$ , where  $\beta$  is the inverse penetration depth.
5. The thermal structure is written by the laser at  $t=0$  for which  $x_0$  is independent of depth, hence  $x'(z, t=0) = x_0$ . As time progresses, a depth dependence  $x'(z, t) = x_0 + G \cdot z \cdot t$  results from the linear velocity profile.
6. The written and subsequently sheared thermal structure is visualized with an infrared imager. This visualization leads to a projection of the 3-d structure to a 2-d temperature distribution. For simplicity and due to the penetration depth of only tens of  $\mu\text{m}$  we model this projection as orthographic.

These model assumptions lead to the following temperature distribution imaged by the infrared camera:

$$T(x, y, t) = T_0 \int_0^\infty e^{-\beta z - \frac{(x-x_0 - Gzt)^2}{\sigma^2}} dz, \quad (1)$$

where  $\beta$  is the absorption coefficient and  $t$  is the time since the thermal structure was written. Solving the integral of this equation leads to

$$T(x, y, t) = T_0 \frac{\sqrt{\pi} \cdot \sigma}{2Gt} e^{\left(\frac{\beta^2 \sigma^2}{4G^2 t^2} - \frac{\beta(x-x_0)}{Gt}\right)} \left(1 + \operatorname{erf}\left[\frac{(x-x_0)}{\sigma} - \frac{\beta}{2Gt}\right] \sigma\right), \quad (2)$$

which can be simplified by introducing  $a = \frac{\sqrt{\pi}}{\beta}$ ,  $b = \frac{\beta}{G \cdot t}$ , and  $c = \frac{\beta \sigma}{2 \cdot Gt}$ :

$$T(x, y, t) = T_0 \cdot ac \cdot e^{(c^2 - b(x-x_0))} \left(1 + \operatorname{erf}\left[\frac{(x-x_0) \cdot b}{2 \cdot c} - c\right]\right). \quad (3)$$

Figure 1 displays a simulation of a sheared heat pattern a time  $t$  after having been written at  $t_0$  viewed from the side. In Figure 2 the time dependence of

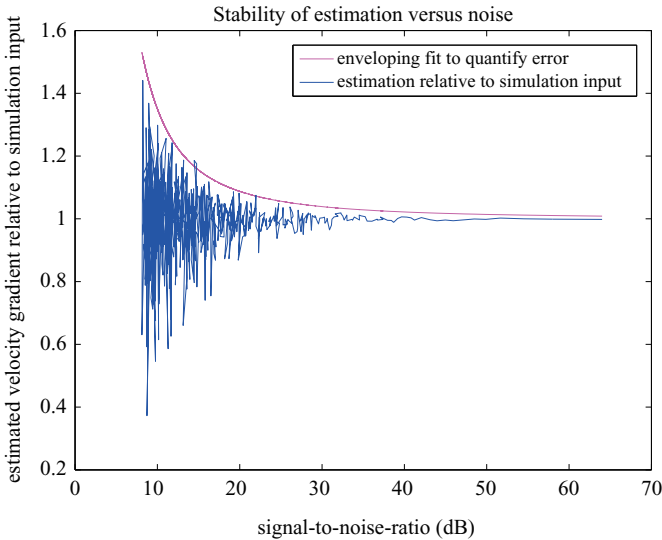


**Figure 3** Results of the accuracy of the proposed technique for simulated data. The ratio of estimated velocity gradient  $G$  to the ground truth value is plotted against the signal-to-noise ratio.

Equation (1) is shown. As expected, the leading edge becomes sharper as time progresses while the trailing edge becomes less well defined.

The velocity gradient  $G$  is computed by performing a non-linear least squares fit to the image data. An exemplary result of such a fit to laboratory data is shown in Figure 4. The gradient  $G$  can be computed from the parameter  $b$  (in Equation (3), as  $\beta$  and  $t$  are well known factors and  $G = \frac{\beta}{b \cdot t}$ .

The new approach of estimating viscous shear contrasts the technique presented by Garbe *et al.* (2007). The new method is not based on motion estimation of active thermographic image sequences. This makes an estimation in single images feasible even at high wind speeds in which the temporal sampling theorem is violated due to large displacements. Also, the data analysis can be performed which significantly less computational cost.

### 3. Experimental Results

To validate our new technique for estimating the viscous shear, we tested it on simulated data. On the simulated data, the new approach performed very well, exhibiting a high accuracy for all the conditions tested. An advantage of testing the approach on simulated data is the ability to perform an analysis of the noise dependence of the approach. For this we added different noise levels of Gaussian

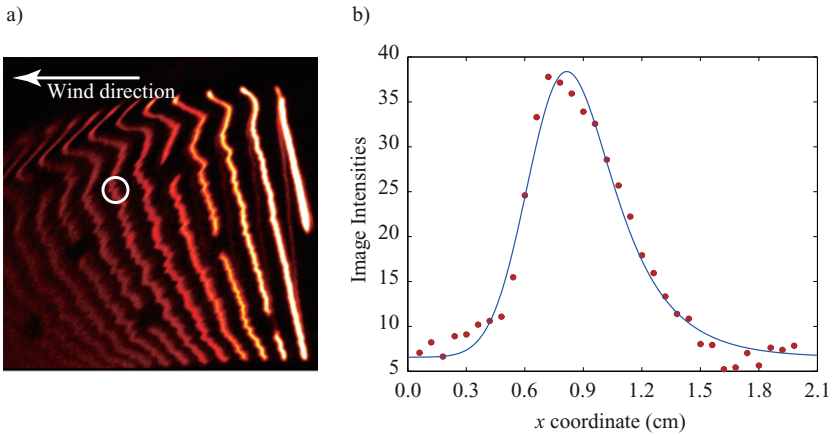


**Figure 4** In a) an infrared image at 7 m/s wind speed can be seen. The area inside the white circle is plotted in b) (points) with the analytical function (solid line) fitted to the data.

noise onto the simulated signal. We present results of the ratio between estimated parameter  $G$  and the ground truth value over noise in Figure 3. It becomes apparent that the error is significant for low signal-to-noise-ratios. However, modern IR cameras exhibit a signal-to-noise ratio of more than 35 dB. At this ratios, the relative error was shown to be in the range of 3 %.

Following the validation on synthetic data, measurements were performed in the Heidelberg Aeolotron and the small Heidelberg wind-wave tank; both are annual wind-wave facilities. A typical image of the measured data and the result of the fitted analytical function from Equation (3) is presented in Figure 4 for 7 m/s wind speed. Conditions were measured from 2 m/s up to 8 m/s. The wind speed was measured at 30 cm above the water surface. Measurements of the friction velocity  $u_{\star}$  were recorded with the spin-down technique and from PIV for comparison. Results of these laboratory measurements are presented in Figure 5.

It can be seen in Figure 5 that laboratory results are not on par with the test on simulated data. The reason for this that precise knowledge of the time  $t$  since writing intensity structures has to be known. During the measurements, the laser and the frames of the IR camera were not synchronized. This has lead to strong uncertainties. Currently, we are conducting more refined experiments with a higher framerate of the IR camera and an accurate synchronization of the  $\text{CO}_2$  laser and the IR camera. Initial tests have shown this to be the main reason for inaccuracies.

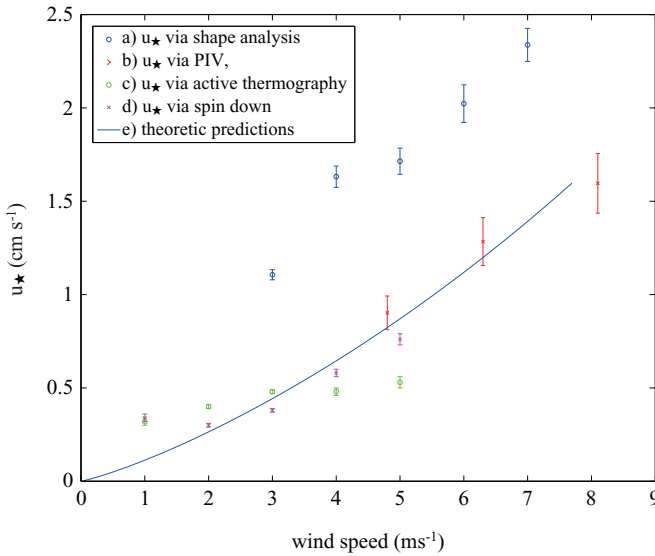


**Figure 5** Comparison of laboratory measurements. The friction velocity measurement  $u_*$  of the presented technique is compared to standard approaches.

## 4. Conclusions

In this contribution we have presented a new technique for measuring viscous shear and the friction velocity due to viscosity from active thermography. A CO<sub>2</sub> laser is used for heating up patches of water. From modeling the temporal change of this temperature pattern, the velocity gradient in the viscous boundary layer can be recovered. From this velocity gradient follows the friction velocity due to viscosity and the viscous shear directly. The analysis is based on a non-linear fit of a derived analytical function to the data. Contrary to previous approaches, no motion estimation or image sequence analysis has to be performed, but the computation can be conducted on individual frames. This greatly reduces the computational cost.

The technique was verified on synthetic data, yielding accuracies of better than 3 % for a signal-to-noise ratio present in modern IR cameras. Additional test measurements were conducted in laboratory facilities. Precise knowledge of the time  $t$  since writing thermal structures with the laser has to be known. This turned out to be the major limitation in currently conducted laboratory experiments. By synchronizing the laser operation with the image acquisition, these limitation will be overcome in future measurements. The technique should be equally applicable

in the field as it is in the laboratory.

### References

- M. A. Atmane, W. Asher, and A. T. Jessup. On the use of the active infrared technique to infer heat and gas transfer velocities at the airwater interface. *Journal of Geophysical Research*, 109:C08S14, 2004. doi: 10.1029/2003JC001805.
- M. L. Banner and W. Peirson. Tangential stress beneath wind-driven air-water interfaces. *Journal of Fluid Mechanics*, 364:115-145, 1998.
- W. S. Broecker and T. H. Peng. Gas exchange rates between air and sea. *Tellus*, 24:21-35, 1974.
- W. S. Broecker and T. H. Peng. *Tracers in the Sea*. Lamont-Doherty Geological Observatory, Columbia University, Palisades, New York, 1982.
- C. S. Garbe, K. Degreif, and B. Jähne. Estimating the viscous shear stress at the water surface from active thermography. In C. S. Garbe, R. A. Handler, and B. Jähne, editors, *Transport at the Air Sea Interface - Measurements, Models and Parametrizations*, pages 223-239. Springer-Verlag, 2007. doi: 10.1007/978-3-540-36906-6\_16.
- H. Haußecker, S. Reinelt, and B. Jähne. Heat as a proxy tracer for gas exchange measurements in the field: Principles and technical realization. In B. Jähne and E. C. Monahan, editors, *Air-Water Gas Transfer - Selected Papers from the Third International Symposium on Air-Water Gas Transfer*, pages 405-413, Heidelberg, 1995. AEON Verlag & Studio Hanau.
- H. Haußecker, U. Schimpf, C. S. Garbe, and B. Jähne. Physics from IR image sequences: Quantitative analysis of transport models and parameters of air-sea gas transfer. In E. Saltzman, M. Donelan, W. Drennan, and R. Wanninkhof, editors, *Gas Transfer at Water Surfaces*, Geophysical Monograph. American Geophysical Union, 2001.
- B. Jähne and H. Haußecker. Air-water gas exchange. *Annual Reviews Fluid Mechanics*, 30: 443-468, 1998.
- B. Jähne, K. O. Münnich, R. Bössinger, A. Dutzi, W. Huber, and P. Libner. On the parameters influencing air-water gas exchange. *Journal of Geophysical Research*, 92 (C2):1937-1949, 1987.
- B. Jähne, P. Libner, R. Fischer, T. Billen, and E. J. Plate. Investigating the transfer process across the free aqueous boundary layer by the controlled flux method. *Tellus*, 41B(2):177-195, 1989.
- T. Kukulka and T. Hara. Momentum flux budget analysis of wind-driven airwater interfaces. *Journal of Geophysical Research*, 110:C12020, 2005. doi: 10.1029/2004JC002844.
- P. S. Liss and L. Merlivat. Air-sea gas exchange rates: Introduction and synthesis. In P. Buat-Menard, editor, *The role of air-sea exchange in geochemical cycling*, pages 113-129. Reidel, Boston, MA, 1986.
- P. S. Liss and P. G. Slater. Flux of gases across the air-sea interface. *Nature*, 247:181-184, 1974. doi: 10.1038/247181a0.
- W. McLeish and G. E. Putland. Measurements of wind-driven flow profiles in the top millimeter of water. *Journal of Physical Oceanography*, 5(3):516-518, 1975. doi: 10.1175/1520-0485(1975)005<0516:MOWDFP>2.0.CO;2.
- J. A. Mueller and F. Veron. Nonlinear formulation of the bulk surface stress over breaking waves: Feedback mechanisms from air- flow separation. *Bound-Lay Meteorol*, 130(1): 117-134, Jan 2009. doi: 10.1007/s10546-008-9334-6.

- K. Okuda, S. Kawai, and Y. Toba. Measurement of skin friction distribution along the surface of wind waves. *J. of Oceanography*, 33(4):190-198, 1977.
- U. Schimpf, C. S. Garbe, and B. Jähne. Investigation of transport processes across the sea surface microlayer by infrared imagery. *Journal of Geophysical Research*, 109(C08S13), 2004. doi: 10.1029/2003JC001803.
- B. M. Uz, M. A. Donelan, T. Hara, and E. J. Bock. Laboratory studies of wind stress over surface waves. *Boundary-Layer Meteorology*, 102(2):301-331, 2002. doi: 10.1023/A:1013119313063.
- R. Wanninkhof. Relationship between gas exchange and wind speed over the ocean. *Journal of Geophysical Research*, 97(C5):7373-7382, 1992.
- R. Wanninkhof and W. R. McGillis. A cubic relationship between gas transfer and wind speed. *Geophysical Research Letters*, 26(13):1889-1892, 1999.
- R. Wanninkhof, W. Asher, R. Wepperning, C. Hua, P. Schlosser, C. Langdon, and R. Sambrotto. Gas transfer experiment on Georges Bank using two volatile deliberate tracers. *J. of Geophys. Res.*, 98(C11):20237-20248, 1993.
- R. Wanninkhof, W. E. Asher, D. T. Ho, C. Sweeney, and W. R. McGillis. Advances in quantifying air-sea gas exchange and environmental forcing. *Annu. Rev. Marine. Sci.*, 1(1):213-244, 2009.
- A. J. Watson, R. C. Upstill-Goddard, and P. S. Liss. Air-sea exchange in rough and stormy seas measured by a dual tracer technique. *Nature*, 349(6305): 145-147, 1991.